Progress In Electromagnetics Research C, Vol. 30, 213–223, 2012

DUAL-BAND DUAL-POLARIZED MICROSTRIP ANTENNA FOR COMPASS NAVIGATION SATELLITE SYSTEM

H. Y. Yuan[1, *], J. Q. Zhang[1], S. B. Qu[1], H. Zhou[1], J. F. Wang[1], H. Ma[1], and Z. Xu[2]

[1]College of Science, Air Force Engineering University, Xi'an 710051, China

[2]Electronic Materials Research Laboratory, Key Laboratory of the Ministry of Education, Xi'an Jiaotong University, Xi'an 710049, China

Abstract—With the development of China's Compass Navigation Satellite System (CNSS), the demand for terminal antennas is quite urgent. In CNSS system, dual-band antennas are more attractive, because they can provide both the navigation and communication functions. In addition, since the CNSS antennas operate at low frequencies, they are not easy to be installed due to their usually large volumes, limiting their practical application. In this paper, we present a dual-band miniaturized CNSS microstrip antenna based on high-permittivity ceramic substrate. This antenna works at S Band (2492 ± 5 MHz, right-handed circular polarization, RHCP) and L Band (1616 ± 5 MHz, left-handed circular polarization, LHCP). Numerical results show that the impedance bandwidth ($S_{11} < -10$ dB), 3 dB axial ratio bandwidth and antenna gain at L Band are about 26 MHz, 6.5 MHz and 3.22 dB, respectively. While the impedance bandwidth ($S_{11} < -10$ dB), 3 dB axial ratio bandwidth and antenna gain at S Band are about 127 MHz, 28 MHz and 4.72 dB, respectively. An experiment was carried out to verify our design and the measured results agree well with the simulation ones. In addition, by using high-permittivity ceramic ($\varepsilon_r = 16$) as the substrate, the antenna keeps its performances with a reduced size by 80% comparing with the conventional ones using low-permittivity substrates. This makes it suitable for practical applications.

Received 17 April 2012, Accepted 13 June 2012, Scheduled 18 June 2012

* Corresponding author: Hang Ying Yuan (yhy1872937@126.com).

1. INTRODUCTION

The Global Positioning System (GPS) is a space-based satellite navigation system that provides location and time information in all weather and anywhere. It plays an important role both in civil and military fields. In addition to GPS, other systems are in use or under development such as the Russian Global Navigation Satellite System (GLONASS), European Union Galileo Positioning System and Chinese Compass Navigation Satellite System. Compared with GPS, CNSS provides not only location and time information, but also communication services. This can be achieved by a dual-band antenna terminate which operates at L Band (1616 $\pm$ 5 MHz, left-handed circularly polarization) to send information and S Band (2492$\pm$ 5 MHz, right-handed circularly polarization) to receive information. Consequently, a demand of dual-band circularly polarized terminal antennas for CNSS has greatly increased. Microstrip patch antennas (MPAs) have irreplaceable advantages in small equipments, especially in portable ones, due to their low profiles, light weight and useful radiation characteristics [1]. They have been widely used in modern communication systems for they can be easily implemented and integrated [2].

In the past two decades, many techniques for the design of patch antennas with multiple-frequency operation have been investigated and proposed. Generally, there are several ways to achieve dual-frequency or multi-frequency performance for MPAs. Firstly, single-layer antenna structure with multiple modes can be used to work at different frequencies. Secondly, single-layer structures with a shorted pin [3] between the radiation patch and the ground, or with slots [4–9], stubs [10, 11] and notches [12] on the patch can be used to control the modes in order to work at dual frequencies. The third way is to use multilayer structures. Since each patch works at a certain frequency [13–15], dual-band antennas can be naturally achieved.

Circularly polarized antennas are more attractive because linearly polarized receiving antenna can only receive part or none of the circularly polarized signal, which significantly lowers the antenna's efficiency. The common methods to get a circularly polarized antenna are to truncate corners [16] or slots on the patches [17–19]. In addition, since the CNSS antennas operate at low frequencies, they are not easy to be installed due to their usually large volumes, limiting their practical application. In view of the aforementioned considerations, in this paper, a dual-band circularly polarized miniaturized patch antenna for CNSS is presented. The dual-band characteristic is achieved by two square patches, and the circular polarization radiations are achieved

by adjusting the size of the slots and the location of feed point. A probe feed is directly connected to the top patch, though a via in the bottom patch. The bottom and top patches perform the L Band, left-handed circularly polarization, and S Band, right-handed circularly polarization. In addition, by using high-permittivity ceramic ($\varepsilon_r = 16$) as the substrate, the antenna keeps its performances with a reduced size by 80% comparing with the conventional ones using low-permittivity substrates. The proposed antenna and results are presented and discussed as follows. In Section 2, the proposed antenna geometry is presented. Simulated results including S_{11}, axial ratio and radiation pattern are given in Section 3. Measured results, analysis and discussion are presented in Section 4. Conclusion is provided in Section 5.

2. ANTENNA DESIGN

The geometry of the dual-band antenna is given in Figure 1. It is composed of two patches which operate at L and S band, respectively. Two square metallic patches are etched on their respective separate substrate with different thicknesses but with the same relative permittivity of $\varepsilon_r = 16$ and loss tangent $\tan\delta = 0.001$. The top patch is directly fed by the center conduction pin of a coaxial connector, while the bottom patch is fed via a circular aperture coupler etched into the bottom metal patch. Slots are etched on the patches to realize right-handed circularly polarization (RHCP) or left-handed circularly polarization (LHCP) states. This lies on the length ratio of the slot in x- and y-directions.

By adjusting the sizes of the patches and feed point, good circularly polarized radiation can be achieved. We utilize a wide aperture coupler whose radial is 1.6 mm for the bottom metal patch feed mechanism in efforts to minimize the sensitivity of the structure to the feed pin position.

To achieve optimal performances, a parametric study is carried out using High Frequency Structure Simulator (HFSS) to investigate the characteristics of the proposed antenna. By the optimization, the geometric dimensions of the proposed antenna are as follows: $a = 40\,\text{mm}$, $L_1 = 13.065\,\text{mm}$, $L_{x1} = 3.4\,\text{mm}$, $L_{y1} = 2.28\,\text{mm}$, $L_2 = 17.97\,\text{mm}$, $L_{x2} = 3.12\,\text{mm}$, $L_{y2} = 2.15\,\text{mm}$, $w = 0.3\,\text{mm}$, and $d = 1.92\,\text{mm}$. The ground plane and the substrate have the square area size of $40\,\text{mm} \times 40\,\text{mm}$.

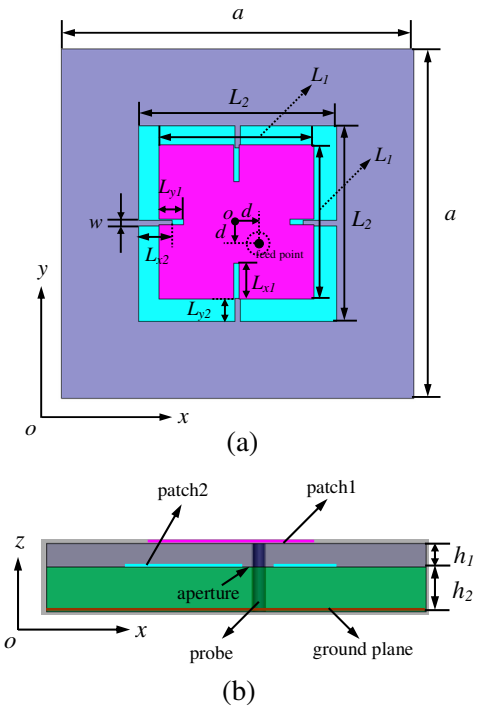

Figure 1. Geometry of the proposed antenna: (a) top view, (b) bottom view.

3. SIMULATION RESULTS USING HFSS

We used the full wave simulation software High Frequency Structure Simulator (HFSS) version 12.0 to calculate its performances. The reflection coefficient (S_{11}) is used in physics and electrical engineering when wave propagation in a medium containing discontinuities is considered. A reflection coefficient describes either the amplitude or the intensity of a reflected wave relative to an incident wave. The reflection coefficient is closely related to the transmission coefficient. The simulated reflection coefficient (S_{11}) at 1.616 GHz as a function of frequency is shown in Figure 2. From Figure 2, we can see that the impedance bandwidth ($S_{11} < -10$ dB) is 26 MHz, and the reflection coefficient at 1.616 GHz is -13.3657 dB. Meanwhile, the $S_{11} < -10$ dB band is from 1.608 GHz to 1.634 GHz.

In Satellite Navigation Systems, the circularly polarized antenna has been widely used, because linear polarized receiving antennas can only receive part or none of the circularly polarized signal, which

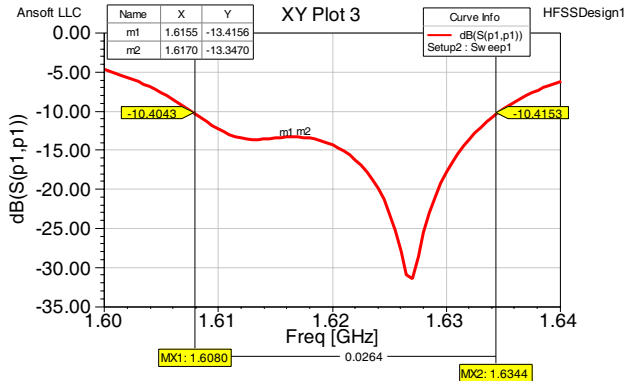

Figure 2. Simulated reflection coefficient (S_{11}) at 1.616 GHz.

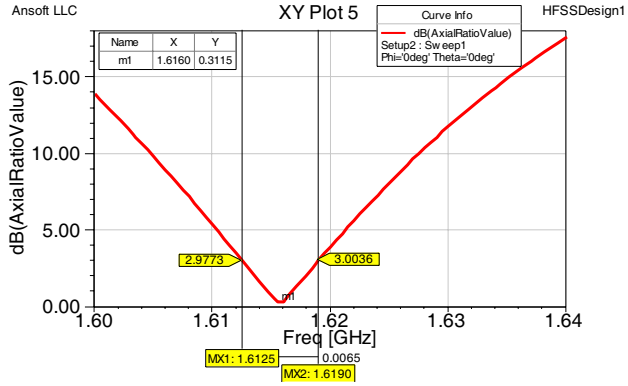

Figure 3. Simulated axial ratio (AR) value at 1.616 GHz.

significantly lowers the antenna's efficiency. However, the circularly polarized signals or antennas can avoid this kind of problems. In general, when the axial ratio is lower than 3 dB, we can consider that this antenna achieves excellent circularly polarized performance. By adjusting sizes of the slots and location of the feed-point, we can achieve excellent circularly polarized performance.

Figure 3 shows the simulated axial ratio (AR) value at 1.616 GHz. Apparently, the 3 dB axial ratio bandwidth is 6.5 MHz, and the axial ratio value at 1.616 GHz is 0.3115 dB. This demonstrates that the proposed antenna has excellent circularly polarized performance.

By changing the location of the feed-point relative to the slots, the proposed antenna can achieve left-handed circularly polarized performance at L Band and right-handed circularly polarized performance at S Band. Figure 4 shows the simulated LHCP and

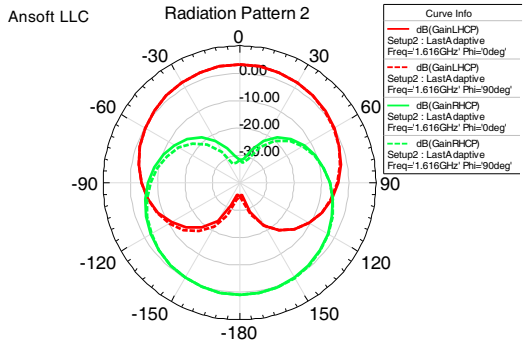

Figure 4. LHCP and RHCP elevation gain patterns of the antenna at 1.616 GHz.

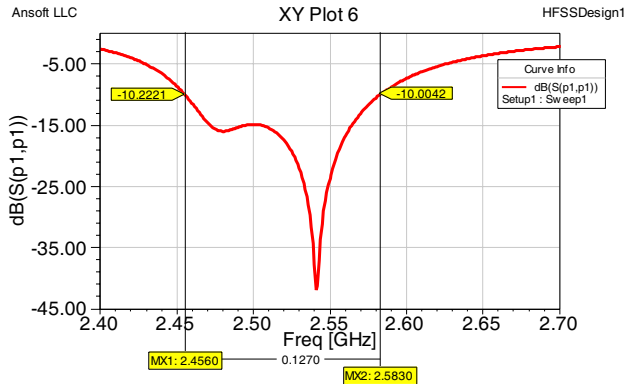

Figure 5. Simulated reflection coefficient (S_{11}) at 2.492 GHz.

RHCP elevation gain patterns of the antenna at 1.616 GHz for $\Phi = 0°$ and $\Phi = 90°$. From Figure 4, we can see that the antenna's left-handed elevation gain is 3.22 dB when $\theta = 0°$. At least 25 dB of gain suppression of the right-handed circular polarization at zenith is achieved. This demonstrates that very little coupling occurs between the lower and upper patch elements. This CNSS antenna achieves excellent left-handed circularly polarized performance at L Band.

The simulated reflection coefficient (S_{11}) at 2.492 GHz as a function of frequency is shown in Figure 5. From Figure 5, we can see that the impedance bandwidth ($S_{11} < -10$ dB) is 127 MHz, and the reflection coefficient at 2.492 GHz is -15.2616 dB. Meanwhile, the $S_{11} < -10$ dB band is from 2.456 GHz to 2.583 GHz.

Figure 6 shows the simulated axial ratio (AR) value at 2.492 GHz. Apparently, the 3 dB axial ratio bandwidth is 28 MHz, and the axial ratio value at 2.492 GHz is 0.3677 dB.

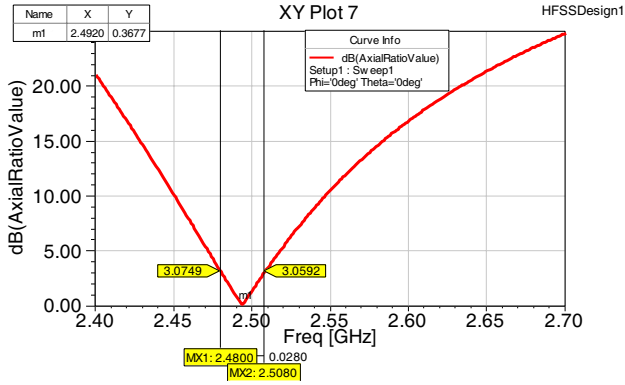

Figure 6. Simulated axial ratio (AR) value at 2.492 GHz.

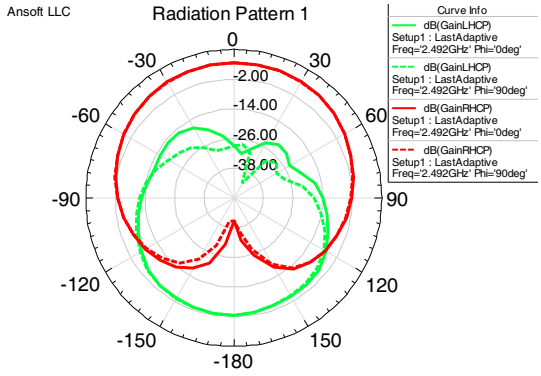

Figure 7. RHCP and LHCP elevation gain patterns of the antenna at 2.492 GHz.

Figure 7 shows the simulated RHCP and LHCP elevation gain patterns of the antenna at 2.492 GHz when $\Phi = 0°$ and $\Phi = 90°$. From Figure 7, we can see that the antenna's right-handed elevation gain is 4.72 dB when $\theta = 0°$. At least 20 dB of gain suppression of the left-handed circular polarization at zenith is achieved. This CNSS antenna achieves excellent right-handed circularly polarized performance at S Band.

4. MEASURED RESULTS

An experiment was carried out to verify our design. Figure 8 shows the prototype of the patch antenna.

Comparison of the simulated and measured reflection coefficient (S_{11}) is given in Figure 9, the solid line is the simulated result curve while the dashed line is the measured result curve. From Figure 9, we can see that this antenna achieves a dual-band function, but the measured resonance frequencies are higher than the simulated results. The measured impedance bandwidth ($S_{11} < -10$ dB) at the lower frequency is 23 MHz, and the $S_{11} < -10$ dB band is from 1.690 GHz to 1.713 GHz; the measured impedance bandwidth ($S_{11} < -10$ dB) at the higher frequency is 148 MHz, and the $S_{11} < -10$ dB band is from 2.793 GHz to 2.931 GHz, respectively.

This discrepancy can be mainly attributed to two factors. Firstly, the permittivity of the fabricated ceramic substrate used in the experiment may be a little lower than 16. Secondly, there is an air-layer between two substrates in the process of conglutinating the two layers. Limited by the experimental equipment conditions, we just give S_{11} of the proposed antenna. In order to determine which factor

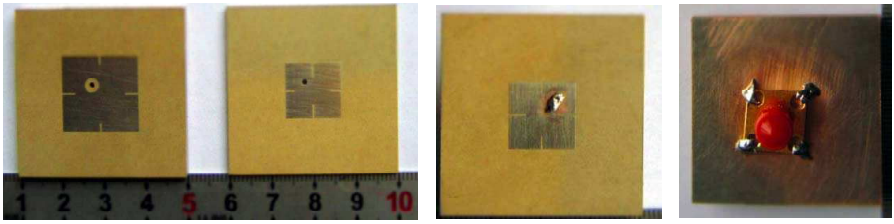

Figure 8. Photograph of the proposed antenna: (a) bottom layer, (b) top layer, (c) top view, (d) bottom view.

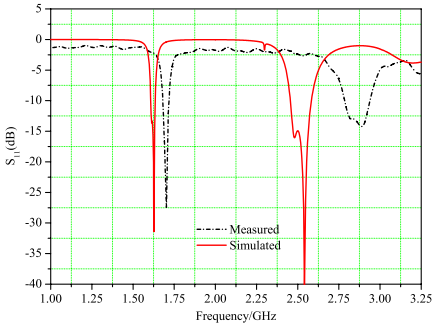

Figure 9. Simulated and measured reflection coefficient (S_{11}).

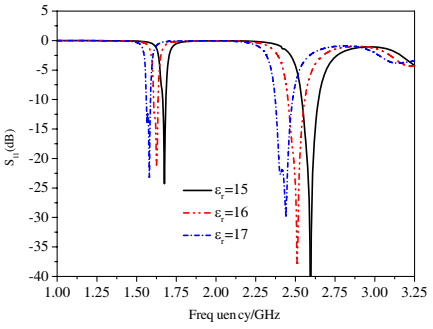

Figure 10. Simulated reflection coefficient (S_{11}) against permittivity ε_r ($\varepsilon_r = 15$, 16, and 17).

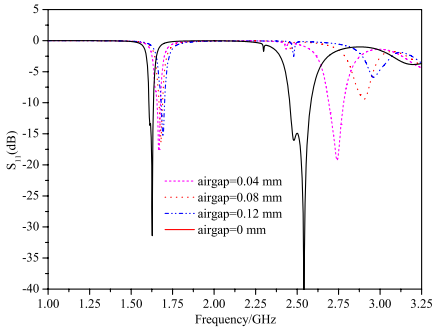

Figure 11. Simulated reflection coefficient (S_{11}) against airgap (airgap = 0 mm, 0.04 mm, 0.08 mm, and 0.12 mm).

mainly causes the discrepancy, we give the simulation analysis results. Figure 10 shows the simulated S_{11} for varied permittivity ε_r = 15, 16 and 17. As the permittivity of the substrate decreases, the two resonances shift to higher frequencies. However, the shifts are quite minor.

Figure 11 shows the simulated S_{11} for airgap = 0 mm, 0.04 mm, 0.08 mm and 0.12 mm. By comparing Figure 9 with Figure 11, we can see that the resonances shift to higher frequencies as the airgap increases. The simulated and measured shifts are quite consistent with each other. Since the relative permittivity of air is 1.0006, the effective permittivity of the substrate is much lower than 16 and thus the resonances shift to higher frequencies.

Comparing the effects of ε_r and airgap on resonant frequencies, we can determine that the discrepancy between the simulated and measured S_{11} is mainly caused by the airgap between the two layers. There are some discrepancies between the simulation and measured results. Nevertheless, this experiment can still prove our design idea.

5. CONCLUSION

We described a stacked patch antenna that is capable of simultaneously sending LHCP L signals and receiving RHCP S signals of CNSS. The CP radiations are achieved by inserting two pairs of narrow slots. Good CP performances are achieved in the two bands. By using high-permittivity ceramic (ε_r = 16) as the substrate, the antenna keeps its performances with a reduced size by 80% comparing with the conventional ones using low-permittivity substrates. The dual-frequency nature of this structure is not limit to the L and S frequency band of CNSS. In general, this design may be scaled and re-optimized

in order to provide a compact, high-performance, single-feed stacked patch antenna for many other sets of two separate frequency bands of interest.

ACKNOWLEDGMENT

This work was supported in part by the National Natural Science Foundation of China under Grants No. 60871027 and in part by National Basic Research Program of China under Grant 2009CB623306 and in part by the Natural Science Foundation of Shaanxi Province of China under Grant No. 2011JQ8031.

REFERENCES

1. Sun, D., W. Dou, L. You, X. Yan, and R. Shen, "A broadband proximity-coupled stacked microstrip antenna with cavity-backed configuration," *IEEE Antennas and Wireless Propagation Letters*, Vol. 10, 1055–1058, 2011.
2. Nakamura, T. and T. Fukusako, "Broadband design of circularly polarized microstrip patch antenna using artificial ground structure with rectangular unit cells," *IEEE Transactions on Antennas and Propagation*, Vol. 59, No. 6, 2103–2110, 2011.
3. Pan, S. C. and K. L. Wong, "Design of dual-frequency microstrip antennas using a shorting-pin loading," *IEEE International Symposium*, 1998.
4. Antar, Y. M. M., A. I. Ittip Iboon, and A. K. Bhattachatyya, "A dual-frequency antenna using a single patch and an inclined slot," *Microwave and Optional Technology Letters*, Vol. 8, No. 6, 309–310, 1995.
5. Gheethan, A. A. and D. E. Anagnostou, "Broadband and dual-band coplanar folded-slot antennas (CFSAs)," *IEEE Transactions on Antennas and Propagation*, Vol. 53, No. 1, 80–89, 2011.
6. Lee, K. F., K. M. Luk, K. M. Mak, and S. L. S. Yang, "On the use of U-slots in the design of dual-and triple-band patch antennas," *IEEE Transactions on Antennas and Propagation*, Vol. 53, No. 3, 60–74, 2011.
7. Bo, L., Y. Guan, Y. Jiang, and A. Zhang, "Compact dual band and circularly polarized microstrip antenna for CNSS," *Cross Strait Quad-regional Radio Science and Wireless Technology Conference*, 401–403, 2011.
8. Sayem, A. T. M. and M. Ali, "Characteristics of a microstrip-fed miniature printed Hilbert slot antenna," *Progress In Electromagnetics Research*, Vol. 56, 1–18, 2006.

9. Tiang, J. J., M. T. Islam, N. Misran, and J. S. Mandeep, "Circular microstrip slot antenna for dual-frequency FRID application," *Progress In Electromagnetics Research*, Vol. 120, 499–512, 2011.
10. Deshmukh, A. A. and K. P. Ray, "Multi-band configurations of stub-loaded slotted rectangular microstrip antennas," *IEEE Antennas and Propagation Magazine*, Vol. 52, No. 1, 89–103, 2010.
11. Heidari, A. A., M. Heyrani, and M. Nakhkash, "A dual-band circularly polarized stub loaded microstrip patch antenna for GPS applications," *Progress In Electromagnetics Research*, Vol. 92, 195–208, 2009.
12. Nakano, H. and K. Vichien, "Dual-frequency patch antenna with a rectangular notch," *Electronics Letters*, Vol. 25, No. 16, 1067–1068, 1989.
13. Ma, S.-L. and J.-S. Row, "Design of single-feed dual-frequency patch antenna for GPS and WLAN applications," *IEEE Transactions on Antennas and Propagation*, Vol. 59, No. 9, 3433–3436, 2011.
14. Pozar, D. M. and S. M. Duffy, "A dual-band circularly polarized aperture-coupled stacked microstrip antenna for global positioning satellite," *IEEE Transaction on Antennas and Propagation*, Vol. 45, No. 11, 1618–1625, 1997.
15. Zhou, Y. J., C. C. Chen, and J. L. Volakis, "Dual band proximity-fed stacked patch antenna for tri-band GPS application," *IEEE Transactions on Antennas and Propagation*, Vol. 55, 220–223, 2007.
16. Yang, S. L. S., K. F. Lee, and A. A. Kishk, "Design and study of wideband single feed circularly polarized microstrip antennas," *Progress In Electromagnetics Research*, Vol. 80, 45–61, 2008.
17. Tian, X.-Q., S.-B. Liu, Y.-S. Wei, and X.-Y. Zhang, "Circularly polarized microstrip antenna with slots for Beidou (COMPASS) navigation system," *Proceedings of International Symposium on Signals, Systems and Electronics*, 2010.
18. Liao, W., Q.-X. Chu, and S. Du, "Tri-band circularly polarized stacked microstrip antenna for GPS and CNSS applications," *ICMMT Proceedings*, 2010.
19. Wu, S.-Q., S.-B. Liu, and Z. Guo, "Coaxial probe-fed circularly polarized microstrip antenna for Beidou RDSS applications," *ICMMT Proceedings*, 2010.